

Note: Integration of trapped ion mobility spectrometry with mass spectrometry

F. A. Fernandez-Lima, D. A. Kaplan, and M. A. Park

Citation: *Rev. Sci. Instrum.* **82**, 126106 (2011); doi: 10.1063/1.3665933

View online: <http://dx.doi.org/10.1063/1.3665933>

View Table of Contents: <http://rsi.aip.org/resource/1/RSINAK/v82/i12>

Published by the [American Institute of Physics](#).

Related Articles

A gain and bandwidth enhanced transimpedance preamplifier for Fourier-transform ion cyclotron resonance mass spectrometry

Rev. Sci. Instrum. **82**, 124101 (2011)

A time of flight mass spectrometer with field free interaction region for low energy charged particle-molecule collision studies

Rev. Sci. Instrum. **82**, 113101 (2011)

A time-of-flight backscattering spectrometer at the Spallation Neutron Source, BASIS

Rev. Sci. Instrum. **82**, 085109 (2011)

A shock tube with a high-repetition-rate time-of-flight mass spectrometer for investigations of complex reaction systems

Rev. Sci. Instrum. **82**, 084103 (2011)

Vacuum compatible sample positioning device for matrix assisted laser desorption/ionization Fourier transform ion cyclotron resonance mass spectrometry imaging

Rev. Sci. Instrum. **82**, 054102 (2011)

Additional information on *Rev. Sci. Instrum.*

Journal Homepage: <http://rsi.aip.org>

Journal Information: http://rsi.aip.org/about/about_the_journal

Top downloads: http://rsi.aip.org/features/most_downloaded

Information for Authors: <http://rsi.aip.org/authors>

ADVERTISEMENT

**AIP**Advances

Submit Now

**Explore AIP's new
open-access journal**

- **Article-level metrics
now available**
- **Join the conversation!
Rate & comment on articles**

Note: Integration of trapped ion mobility spectrometry with mass spectrometry

F. A. Fernandez-Lima,^{1,a)} D. A. Kaplan,² and M. A. Park²

¹Department of Chemistry, Texas A&M University, College Station, Texas 77843-3144, USA

²Bruker Daltonics, Inc., Billerica, Massachusetts 01821, USA

(Received 22 August 2011; accepted 14 November 2011; published online 8 December 2011)

The integration of a trapped ion mobility spectrometer (TIMS) with a mass spectrometer (MS) for complementary fast, gas-phase mobility separation prior to mass analysis (TIMS-MS) is described. The ion transmission and mobility separation are discussed as a function of the ion source condition, bath gas velocity, analysis scan speed, RF ion confinement, and downstream ion optical conditions. TIMS mobility resolution depends on the analysis scan speed and the bath gas velocity, with the unique advantage that the IMS separation can be easily tuned from high speed (~ 25 ms) for rapid analysis to slower scans for higher mobility resolution ($R > 80$). © 2011 American Institute of Physics. [doi:10.1063/1.3665933]

Ion mobility spectrometry (IMS) coupling to mass spectrometry offers several advantages over traditional mass spectrometry (MS), including separation of ions from mixtures based on composition and charge state, the ability to separate geometric isomers, increased dynamic range, and discrimination against chemical noise.¹ Several research groups have focused on achieving high resolution IMS separation ($R > 50$) as this factor mainly limits the information that can be experimentally derived. In a different IMS approach, the use of a trapped ion mobility spectrometer (TIMS) device for fast, gas-phase separation of molecular isobar pairs has been recently described.¹ In the present note, we describe the TIMS-MS integration and its advantage over traditional drift tube based IMS-MS designs; discussion is also focused on the factors that influence TIMS-MS mobility separation, dynamic range, and versatility.

In the example presented here, ions were generated by electrospray ionization (ESI) using an ESI ion source based on the Apollo II design (Bruker Daltonics Inc., MA). Accordingly, a quadrupole funnel optic was used and the capillary coupling the ESI spray chamber to the first pumping stage was orthogonal to the axis of the TIMS analyzer. Each TIMS electrode is composed of four electrically isolated segments. In the entrance and exit funnel sections, a RF-induced pseudo-potential keeps the ions away from the funnel walls (180° out of phase between adjacent plates). However, in the analyzer section, the phase of the RF potential does not alternate between adjacent plates but only between adjacent segments. The RF field (typically 950 kHz and 200–400 Vpp) plays little or no direct role in the mobility analysis. The operating pressure difference ($P1 = 2.6$ – 3.4 and $P2 = 2.6$ mbars) produces a cylindrically symmetric gas flow of nitrogen at ~ 300 K. After exiting the TIMS analyzer, ions are focused, using a series of lenses and a hexapole ion guide, through the main differential pumping region. In this transfer area, residual pressure drops from 2.6 mbars in the first funnel to 10^{-4} mbars in the

hexapole. After the transfer area, ions enter the quadrupole mass analyzer (Q), which can be operated in transmission or isolation mode. Ions exiting the Q are injected into the collision cell and ion cooling cell regions. The collision and ion cooling cells have a hexapole and quadrupole structure, respectively. The hexapole collision cell was driven at a RF frequency and amplitude of about 1 MHz and 600 Vpp, whereas the quadrupole ion cooler was operated at a frequency and amplitude of 2 MHz and 600 Vpp. The plates of the collision and ion cooler cells are connected by a network of precision resistors operating as a voltage divider. A DC potential across the resistor divider results in a corresponding axial electric field across the cells. The ToF analyzer is composed of an ion pulsed extraction region, a two stage reflectron, and a MCP-based detector (see Figure 1(a)). The oToF analyzer was operated at 5–10 kHz, with a total ion acceleration voltage of about 10 kV (mass resolution 10–15 k). Molecules used in this study were purchased from Sigma (St. Louis, MO) and used as received. Samples were electrosprayed at a concentration of 1–10 μM in a 1:1 (v/v) water/methanol solution. An electrosprayed Tuning Mix calibration standard (Tunemix, G2421A) was purchased from Agilent Technologies (Santa Clara, CA) and used as received. Details on the Tunemix structures (e.g., $m/z = 322, 622, \text{ and } 922$) can be found in Ref. 2.

The elution voltage, and therefore resolution depends on the velocity of the bath gas: higher velocity implies a higher elution voltage and a higher mobility resolution ($R = K/\Delta K = (V_{\text{out}} - V_{\text{elut}})/\Delta V$). A higher gas velocity can be achieved, in practice, by varying the P1 and P2 pressure – the limiting factor in the gas velocity being the pumping speed at the interface. TIMS mobility resolution also depends on the electric field ramp speed ($\Delta V_{\text{ramp}}/T_{\text{ramp}}$) – slower ramp speeds lead to higher resolutions. In practice, the ramp speed is reduced by decreasing the ramp range, ΔV_{ramp} , and/or increasing the ramp time, T_{ramp} (see example in Figure 1(b)). As the bath gas pressure increases in the entrance region (P1), the bath gas velocity also increases leading to an increase in the TIMS mobility resolution. Moreover, as the T_{ramp} increases the ramp speed decreases and a higher mobility resolution is obtained.

^{a)} Author to whom correspondence should be addressed. Electronic mail: ffernandez@chem.tamu.edu.

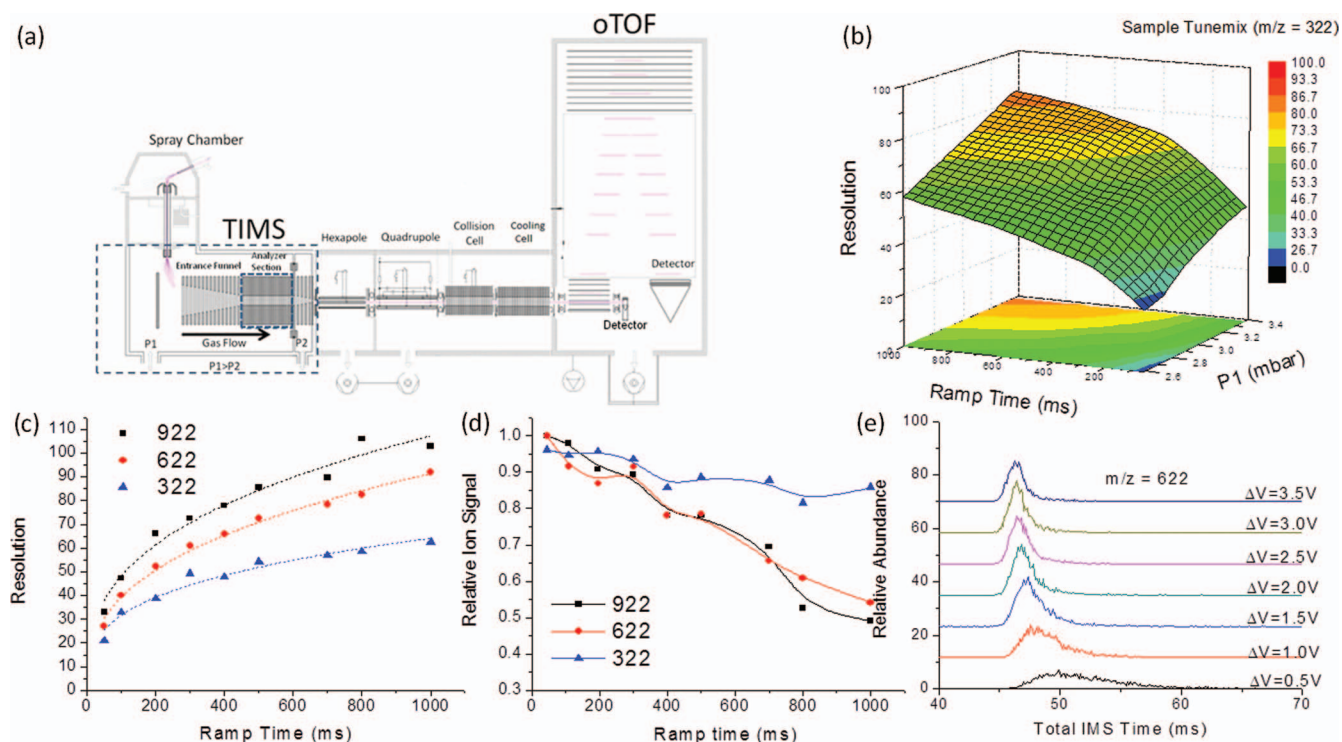


FIG. 1. (Color online) (a) TIMS-MS instrument schematics. (b) Mobility resolution dependence on the ramp time and the inlet pressure P1. (c) Mobility resolution dependence on the ramp time for a Tunemix mixture ($m/z = 322$, 622, and 922). (d) Relative ion signal dependence on the ramp time. (e) Total IMS time dependence on the axial field applied on the ion cooling cell.

TIMS mobility resolution has a similar dependence on the electric field strength as that in a traditional drift tube. Notice that higher size-to-charge ratio ions are trapped and eluted at higher electric field strengths; that is, they are separated with a higher mobility resolution (see example in Figure 1(c)). As the ramp time increases, ion signal may decrease – perhaps due to the neutralization or scattering of the ions (see example in Figure 1(d)). Thus, a balance may be struck between resolution and signal intensity. It is important to notice that the mobility resolution also depends on the ion optics following the TIMS analyzer – i.e., the hexapole, Q, and collision and cooling cells. For example, Figure 1(e) shows the variation of the IMS time as a function of the axial field applied across the cooling cell. With the increase in the axial field the IMS resolution also increases. A practical limit in the axial field is defined by the fragmentation energy of the ions of interest. Notice that in a TIMS-MS device ions elute from low to high mobilities, contrary to conventional drift tube based IMS-MS analyzers. That is, in TIMS-MS larger size ions elute first, and more compact ions elute later. The axial field across the MS sections is important to guarantee the correlation between the TIMS elution step and the MS detection. There are a number of experimental conditions that can affect the performance of a TIMS-MS device. In the case of an ESI source, the analyte desolvation can be affected by the temperature and flow rate of the drying gas (nitrogen in our case). For example, no variation in the total IMS time was observed as a function of the drying gas flow rate (Tunemix mixture, 2–10 $\mu\text{l}/\text{min}$ flow rate range) That is, the apparent mobilities of the peaks did not change. Nevertheless, ion signal intensity depends on the flow

rate; for the example shown, the optimal dry gas flow rate was found to be 6 $\mu\text{l}/\text{min}$. For RF linear devices, it is well known that the efficiency of radial confinement varies with m/z . For a TIMS device, a small dependence on the RF amplitude allows the analysis of a wide range of m/z in a single scan. The signal intensity dependence on RF was studied for a Tunemix mixture ($m/z = 322$, 622, and 922). In the range studied, as the RF amplitude increases, the ion signal varies as a function of m/z (Figure 2(a)). For lower RF amplitudes, ions of low m/z are better confined and transmitted. With the increase of the RF amplitude, higher m/z ion signals increase. For practical purposes, a good compromise is found at $V_{pp} = 300$ V for a mass range $m/z = 200$ –1000. The variation of the ion packet size trapped in a TIMS analyzer may also influence the TIMS-MS performance. For example, the ion packet size can be experimentally varied by the number of ions injected into the mobility analyzer region (fill time). Figure 2(b) shows the variation of the ion signal as a function of the fill time. As the fill time increases, the ion signal increases until a saturation point (~ 50 ms). The saturation point depends on the ion concentration in the ESI beam. In the example shown here, the highest intensity is observed for $m/z = 622$, which reaches a saturation before $m/z = 322$ and 922 (this is also observed in transmission mode MS analysis). Coulombic repulsion increases with the ion density increase leading to an effective increase of the ion radial motion inside the mobility analyzer region, reaching a saturation point. The Coulombic repulsion can also lead to a broadening of the IMS peak. Under the conditions studied here there was no variation in the elution voltage with the ion density. Further experiments will focus on

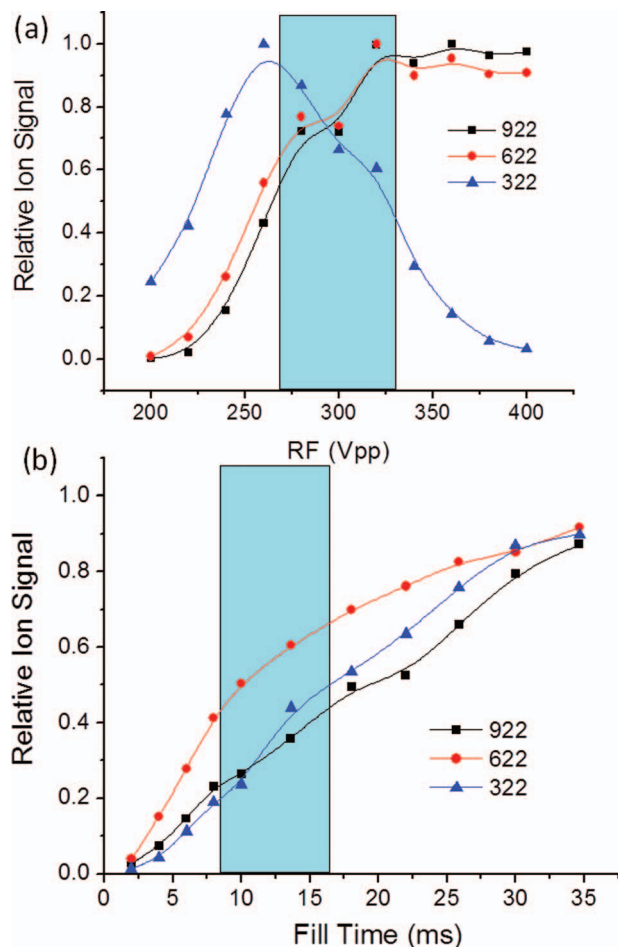


FIG. 2. (Color online) Relative ion signal variation for a Tunemix sample ($m/z = 322, 622,$ and 922) as a function of (a) RF amplitude and (b) fill time.

the perturbation of the ion radial motion due to the ion density as well as the influence of co-trapped ion packages with different mobilities.

TIMS voltages were defined using National Instruments data acquisition cards (NI-PXI-6704, NI-PXI-6289, NI-PXI-6361) and a 1 GHz digitizer (NI-PXI-5154) was used for the MS data acquisition. All cards were housed in a 1073e PXI chassis, operated off a computer PXIe extension bus. The IMS-MS experiment was synchronized with the TOF start (extraction trigger). The digitizer trigger was internally routed

through the PXI chassis and sent to the PXI-6361. A digital pattern was then output at a rate of 10 MHz which was triggered by the routed digitizer trigger. The digital pattern, defined by the user, consisted of three transistor-transistor logic triggers which were used for: (1) trapping ions in the TIMS analyzer section, (2) blocking ions from entering the TIMS analyzer section, and (3) signaling the start of the voltage ramp in the TIMS analyzer section for ion elution. The ramp voltage was controlled by the PXI-6289 analog output (AO). The ramp voltage range (V_{ramp}) and time (T_{ramp}) were defined in the software and built as an array of output voltages. The output voltage of the PXI-6289 (± 10 V AO) was amplified using an in-house $15\times$ amplifier capable of 50 kHz ramp rates. The internally routed trigger was also used as the output clock of the PXI-6289, which results in the TIMS voltage steps synchronized with the TOF pulses. Notice that MS data was acquired from the digitizer for each ramp step (i.e., 1 record set at a time). After a full set of IMS records were acquired from the digitizer, all of the PXI cards were reset and the next TOF trigger restarted the process again. This acquisition process (i.e., re-initializing the cards) was required due to the slow data transfer rate from the digitizer to the computer and to ensure proper timing synchronization during the entire IMS-MS experiment separation.

The integration of TIMS with MS creates a powerful analytical tool for complementary size-to-charge and mass-to-charge separation. TIMS-MS has the unique advantage that it performs IMS separations based not on time – e.g., drift time – but on elution voltage. Thus, TIMS-MS has added flexibility over conventional IMS in that the speed and range over which the voltage (mobility) is scanned can be readily adjusted according to the requirements of the application – i.e., speed vs. range vs. resolution.

This work was supported by the National Institute of Health (Grant No. 1K99RR030188-01) and a 2010&2011 Bruker Daltonics, Inc. Fellowship. The authors would like to acknowledge Anita Salmon, Lauren Lasseter, and John Bongarts from National Instruments for their helpful discussions and technical support.

¹F. A. Fernandez-Lima, D. A. Kaplan, J. Suetering, and M. A. Park, *Int. J. Ion Mobility Spectrosc.* **14**, 93 (2011), and references herein

²L. A. Flanagan, U. S. patent 5872357, Hewlett-Packard Company, Palo Alto, CA, USA, February 16, 1999, p. 19.